Oxidative Addition of MeI to a Rhodium(I) N-Heterocyclic Carbene Complex. A Kinetic Study

Helen C. Martin, Neil H. James, John Aitken, Joseph A. Gaunt, Harry Adams, and Anthony Haynes*

Department of Chemistry, University of Sheffield, Sheffield, S3 7HF, U.K.

Received July 7, 2003

The Rh(I) iodocarbonyl complexes [Rh(CO)(L_{Me})$_2$I] (**3a**) and [Rh(CO)(L_{Mes})$_2$I] (**3f**) (L_{Me} = 3,5-dimethylimidazoline-2-ylidene; L_{Mes} = 3,5-dimesitylimidazoline-2-ylidene) have been prepared by the reaction of [Rh(CO)$_2$(OAc)]$_2$ or [Rh(CO)$_2$(acac)] with an imidazolium salt in the presence of Cs_2CO_3. Complex **3a** reacts with MeI to give a Rh(III) acetyl complex, [Rh(L_{Me})$_2$I$_2$(COMe)] (**5a**), which is unstable and decomposes by elimination of MeI to regenerate **3a**. Rate and equilibrium constants have been measured for the reversible reaction **3a** + MeI → **5a**. Thermodynamic parameters indicate that the forward reaction is exothermic ($\Delta H = -51 \pm 3$ kJ mol^{-1}) but disfavored entropically ($\Delta S = -159 \pm 12$ J mol^{-1} K^{-1}). Complex **3f** does not react with MeI. The results are compared with data reported for [Rh(CO)(PEt$_3$)$_2$I], and the differences in behavior of the N-heterocyclic carbene and PEt$_3$ systems are interpreted on the basis of ligand steric effects. An X-ray crystal structure is presented for [Rh(L_{Me})$_2$I$_2$(OAc)] (**6a**), and a mechanism is proposed for its formation from **5a**. Tests on **3a** as a catalyst for the carbonylation of methanol indicate sequential loss of the two L_{Me} ligands and formation of [Rh(CO)$_2$I$_2$]$^-$.

Introduction

Since the isolation in 1991 of a free N-heterocyclic carbene (NHC) by Arduengo et al.,[1] there has been a rapid growth in the use of NHCs as ligands in transition metal chemistry. The synthesis and properties of this class of complexes have been the subject of several recent reviews.[2−5] The donor power of NHC ligands is considered to be greater than that of phosphines, prompting a range of investigations seeking to exploit their properties in homogeneous catalysis. Perhaps of most significance are the Ru-based olefin metathesis catalysts developed by Grubbs et al.[6] and Pd- or Ni-based catalysts for C−C coupling reactions.[3] Other catalytic processes for which NHC complexes have shown activity include hydroformylation, CO/alkene copolymerization, hydrosilylation, and hydrogenation.

Despite the intense interest in the catalytic properties of NHC complexes, there have been relatively few quantitative studies of the fundamental reaction steps in their catalytic cycles. Calorimetric measurements by Nolan et al. gave reaction enthalpies for coordination of NHC ligands to the Cp*RhCl moiety, which indicated NHCs to have a higher donor strength than trialkylphosphines.[7,8] Simms et al. measured equilibrium constants for substitution of the phosphine in [CpCo(PPh$_3$)Me$_2$] by an NHC ligand.[9] In both of these systems, steric effects of N-substituents on the NHC ligands were found to be significant. A kinetic study of decomposition of Pd(Me)(NHC) complexes via reductive elimination has also been reported.[10]

Oxidative addition is a fundamental class of organometallic reaction which plays a key role in many catalytic processes. Much of the quantitative understanding of oxidative addition has arisen from studies of the reactivity of Vaska-type complexes, [M(CO)L$_2$X] (M = Rh, Ir; L = PR$_3$; X = halide, pseudohalide). The electronic and steric properties of L are both important for the reaction kinetics and thermodynamics, oxidative addition being favored by small, strongly basic phosphines such as PMe$_3$. Vaska-type complexes containing L = NHC were first reported in the 1970s,[11−13] and although some oxidative addition chemistry has been reported, there has been no quantitative comparison of the reactivities of [M(CO)(PR$_3$)$_2$X] and [M(CO)(NHC)$_2$X].

* Corresponding author. E-mail: a.haynes@sheffield.ac.uk.

(1) Arduengo, A. J., III; Harlow, R. L.; J, K. M. *J. Am. Chem. Soc.* **1991**, *113*, 361.
(2) Herrmann, W. A.; Kocher, C. *Angew. Chem., Int. Ed. Engl.* **1997**, *36*, 2162. Weskamp, T.; Bohm, V. P. W.; Herrmann, W. A. *J. Organomet. Chem.* **2000**, *600*, 12.
(3) Herrmann, W. A.; Weskamp, T.; Volker, P. W. B. *Adv. Organomet. Chem.* **2002**, *48*, 1. Herrmann, W. A. *Angew. Chem., Int. Ed.* **2002**, *41*, 1290.
(4) Bourrissou, D.; Guerret, O.; Gabbai, F. P.; Bertrand, G. *Chem. Rev.* **2000**, *100*, 39.
(5) Jafarpour, L.; Nolan, S. P. *Adv. Organomet. Chem.* **2001**, *46*, 181.
(6) Trnka, T. M.; Grubbs, R. H. *Acc. Chem. Res.* **2001**, *34*, 18.
(7) Huang, J.; Schanz, H.-J.; Stevens, E. D.; Nolan, S. P. *Organometallics* **1999**, *18*, 2370.
(8) Huang, J.; Stevens, E. D.; Nolan, S. P.; Petersen, J. L. *J. Am. Chem. Soc.* **1999**, *121*, 2674.
(9) Simms, R. W.; Drewitt, M. J.; Baird, M. C. *Organometallics* **2002**, *21*, 2958.
(10) McGuinness, D. S.; Saendig, N.; Yates, B. F.; Cavell, K. J. *J. Am. Chem. Soc.* **2001**, *123*, 4029.
(11) Hartshorn, A. J.; Lappert, M. F.; Turner, K. *J. Chem. Soc., Dalton Trans.* **1978**, 348. Cetinkaya, B.; Dixneuf, P.; Lappert, M. F. *J. Chem. Soc., Dalton Trans.* **1974**, 1827. Cardin, D. J.; Doyle, M. J.; Lappert, M. F. *J. Organomet. Chem.* **1974**, *65*, C13. Lappert, M. F. *J. Organomet. Chem.* **1988**, *358*, 185.
(12) Doyle, M. J.; Lappert, M. F. *J. Chem. Soc., Chem. Commun.* **1974**, 679.
(13) Lappert, M. F.; Pye, P. L. *J. Chem. Soc., Dalton Trans.* **1977**, 2172.

10.1021/om034022g CCC: $25.00
Publication on Web 09/25/2003

Chart 1. Rh Chlorocarbonyl Vaska Analogues Containing NHC Ligands[a]

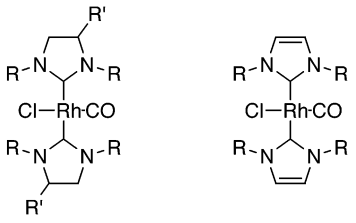

1a-e **2a,f**

[a] R, R′ = (a) Me, H; (b) Et, H; (c) Et, ^{t}Bu; (d) CH_2Ph, H; (e) 4-pentenyl, H; (f) mesityl, H.

Scheme 1. Synthesis of 3a

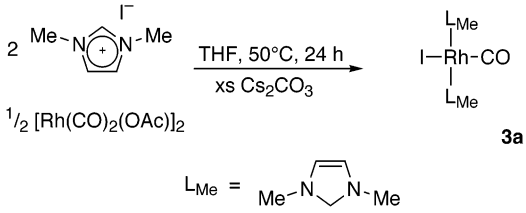

3a

In this paper we report a kinetic study of the oxidative addition of methyl iodide to a Rh(I) Vaska analogue containing NHC ligands and compare the results with those in the literature for related phosphine systems.

Results and Discussion

Synthesis of Rh(I)-NHC Complexes. A number of rhodium(I) chlorocarbonyl Vaska analogues, $[Rh(CO)(NHC)_2Cl]$ (**1a**−**e**, **2a**,**f**), have been reported in the literature. Nearly 30 years ago, Lappert and co-workers developed a synthetic route to the saturated imidazolidine-2-ylidene complexes (**1a**−**d**) involving reaction of the appropriate enetetramine with $[Rh(CO)_2Cl]_2$.[11,12,14,15] An alternative route to complexes **1b**,**d**,**e** involving NHC ligand transfer from $[W(CO)_5(NHC)]$ has been reported by Liu and co-workers.[16] Complexes **2a**,**f**, containing unsaturated imidazoline-2-ylidene ligands, were prepared via complexation of the free carbene ligand to Rh(I)[17,18] followed by carbonylation.

For our studies of MeI oxidative addition, we elected to use Rh(I) iodocarbonyl complexes to avoid potential complications arising from a mixed halide system. Our synthetic route to $[Rh(CO)(L_{Me})_2I]$ (**3a**) employs in situ formation of the carbene ligand from an imidazolium salt, as illustrated in Scheme 1.

The Rh(I) precursor $[Rh(CO)_2(OAc)]_2$ was chosen since its acetate ligands could potentially deprotonate the imidazolium cation. However, to generate the required 2 equiv of NHC ligand per Rh center, it was necessary to add an external base. Cesium carbonate proved to be significantly more effective than sodium carbonate in this role, possibly due to higher solubility in the reaction medium. A mononuclear Rh(I) reactant, $[Rh(CO)_2(acac)]$, was also found to give **3a** under the conditions shown in Scheme 1.

Scheme 2. Reaction of 3a with MeI

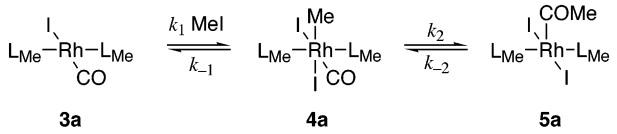

3a **4a** **5a**

The ^{1}H NMR spectrum of **3a** closely resembles that reported for the chloride analogue, **2a**, with singlets for both the *N*-methyl and olefinic protons of the NHC ligands. This very simple spectrum is consistent with a trans geometry, which makes the two L_{Me} ligands equivalent, as in the X-ray crystal structure reported for **2a**.[17] The IR spectrum of **3a** (in CH_2Cl_2) shows a ν(CO) absorption at 1943 cm^{-1}, indicating relatively high electron density on the Rh(I) center. When the preparative reaction was conducted at room temperature rather than 50 °C, additional ν(CO) absorptions were observed at 2074 and 2001 cm^{-1}. These bands are assigned to an intermediate dicarbonyl species, $[Rh(CO)_2(L_{Me})I]$, which has previously been reported as the product of the reaction of $[Rh(CO)_2(acac)]$ with 1,3-dimethylimidazolium iodide in the *absence* of external base.[19]

When 1,3-dimesitylimidazolium chloride was used as the ligand precursor, excess cesium iodide was added to the reaction mixture in order to favor formation of the iodide product, $[Rh(CO)(L_{Mes})_2I]$ (**3f**). The ^{1}H NMR spectrum of **3f** resembles that reported for the chloride analogue, **2f**, with two resonances for the ortho-methyl substituents of the *N*-mesityl groups, indicating restricted rotation about the mesityl−N bonds. The ν(CO) band at 1937 cm^{-1} suggests that the L_{Mes} ligands in **3f** are slightly better donors than the L_{Me} ligands in **3a**.

Reaction of Rh(I) Complexes with Methyl Iodide. On the basis of the low ν(CO) frequencies observed for **3a** and **3f**, relatively high nucleophilicity toward MeI was envisaged. However, treatment of **3a** with a large excess of MeI in CH_2Cl_2 at 25 °C resulted in a rather slow reaction. The product had an IR absorption at 1697 cm^{-1}, indicative of a Rh(III)-acetyl complex, **5a**, resulting from facile migratory CO insertion in **4a** after oxidative addition of MeI (Scheme 2). At concentrations of MeI up to 8 M, formation of the acetyl product **5a** did not go to completion, indicating facile reversibility of the reaction sequence shown in Scheme 2. On removal of the excess MeI and dissolution of the residue in CH_2Cl_2, IR spectroscopy indicated the re-formation of **3a** from **5a**.

Although the instability of **5a** precluded its isolation as a pure compound, its reversion to **3a** could also be followed by ^{1}H NMR spectroscopy. A sample containing mostly **5a** was generated by reaction of **3a** with neat (16 M) MeI, which was removed in vacuo. The sample was then dissolved in CD_2Cl_2 in an NMR tube, and spectra were recorded at intervals over a period of 8 h. The ^{1}H NMR spectrum of **5a** displayed a singlet at δ

(14) Cetinkaya, B.; Hitchcock, P. B.; Jasim, H. A.; Lappert, M. F. *NATO ASI Ser., Ser. C* **1989**, *269*, 59. Coleman, A. W.; Hitchcock, P. B.; Lappert, M. F.; Maskell, R. K.; Muller, J. H. *J. Organomet. Chem.* **1985**, *296*, 173.

(15) Cetinkaya, B.; Hitchcock, P. B.; Lappert, M. F.; Shaw, D. B.; Spyropoulos, K.; Warhurst, N. J. W. *J. Organomet. Chem.* **1993**, *459*, 311.

(16) Ku, R.-Z.; Huang, J.-C.; Cho, J.-Y.; Kiang, F.-M.; Reddy, K. R.; Chen, Y.-C.; Lee, K.-J.; Lee, J.-H.; Lee, G.-H.; Peng, S.-M.; Liu, S.-T. *Organometallics* **1999**, *18*, 2145. Liu, S.-T.; Hsieh, T.-Y.; Lee, G.-H.; Peng, S.-M. *Organometallics* **1998**, *17*, 993.

(17) Herrmann, W. A.; Fischer, J.; Ofele, K.; Artus, G. R. J. *J. Organomet. Chem.* **1997**, *530*, 259.

(18) Huang, J.; Stevens, E. D.; Nolan, S. P. *Organometallics* **2000**, *19*, 1194.

(19) Herrmann, W. A.; Elison, M.; Fischer, J.; Kocher, C.; Artus, G. R. J. *Chem. Eur. J.* **1996**, *2*, 772.

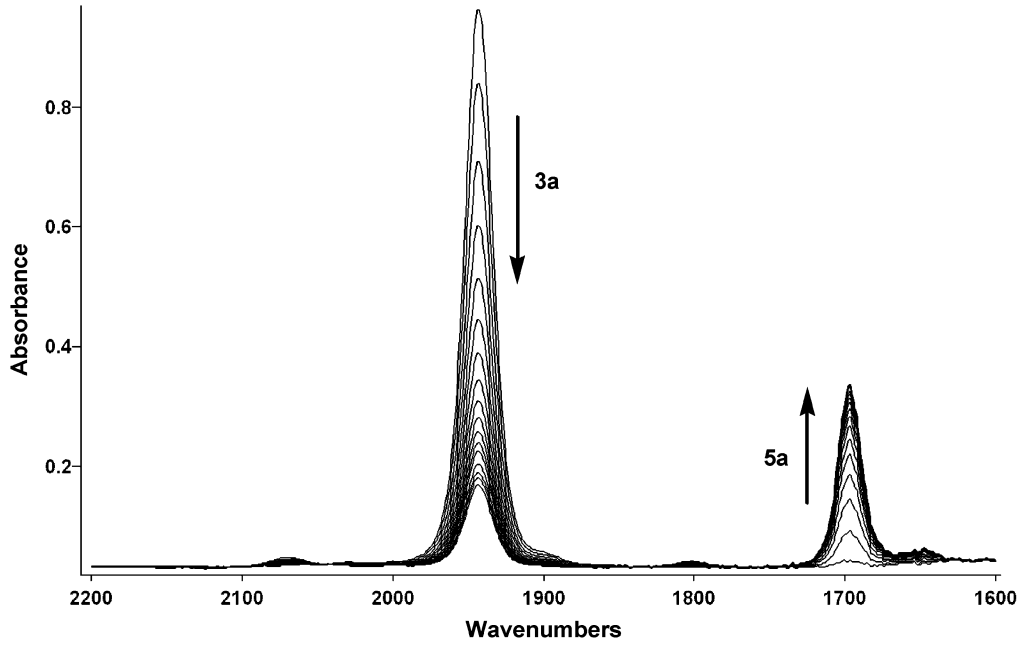

Figure 1. Series of IR spectra recorded during the reaction of **3a** with MeI.

3.17 due to acetyl ligand and singlets at δ 3.73 and 3.93 associated with inequivalent *N*-methyl groups on the NHC ligands. A pair of doublets ($^3J_{HH}$ 1.5 Hz) at δ 6.97 and 7.03 indicated inequivalent NHC olefinic protons. The spectrum provides evidence for restricted rotation about the Rh−L_{Me} bonds as found in a number of other NHC complexes.[12,20] Although the spectroscopic data do not provide definitive structural characterization of **5a**, they are consistent with a square-pyramidal geometry with an apical acetyl ligand proposed in Scheme 2, as found for a number of other five-coordinate Rh(III)-acetyl complexes of the form [RhL_2X_2(COMe)].[21−23] However, we cannot rule out the possibility that **5a** exists as an iodide-bridged dimer. The trans configuration shown for **5a** in Scheme 2 is also uncertain, but quite likely in view of the equilibrium with the trans complex **3a**. Over time, all the ^{1}H NMR resonances of **5a** decayed in proportion, with the concomitant growth of singlets due to **3a** at δ 3.95 and 6.96 and MeI at δ 2.16. The mesityl-substituted complex **3f** was found to be completely unreactive with MeI. Even when dissolved in neat MeI, no decay of the reactant was observed over 24 h.

Kinetic Measurements. FTIR spectroscopy was employed to monitor the reaction of **3a** with MeI in CH_2Cl_2 as a function of temperature and [MeI]. Pseudo-first-order conditions were maintained by keeping the [MeI] in large excess compared with [Rh]. Figure 1 shows a typical series of spectra, in which the band due to **3a** decays and that due to **5a** grows until equilibrium is attained. Absorbance versus time plots for these two bands are shown in Figure 2. The data are well fitted by exponential curves, from which pseudo-first-order rate constants (k_{obs}) for the approach to equilibrium can be obtained (Table 1).

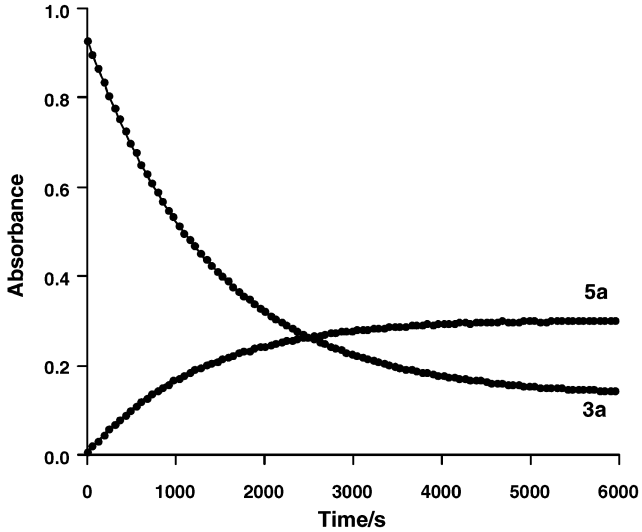

Figure 2. Kinetic plot showing growth and decay of ν(CO) bands of **3a** and **5a** during reaction of **3a** with MeI (1.6 M in CH_2Cl_2, 25 °C).

$$\mathbf{3a} + \mathrm{MeI} \underset{k_b}{\overset{k_f}{\rightleftharpoons}} \mathbf{5a} \quad (1)$$

$$k_{obs} = k_f[\mathrm{MeI}] + k_b \quad (2)$$

The simplified reaction scheme shown in eq 1 leads to the expression for k_{obs} given in eq 2. Consistent with this, a plot of k_{obs} versus [MeI] at 25 °C gives a reasonable linear fit ($R = 0.996$), and the slope provides a value for the net forward rate constant, $k_f = (3.0 \pm 0.1) \times 10^{-4}$ M^{-1} s^{-1}. Closer inspection of the k_{obs} versus [MeI] plot reveals a slight deviation from linearity, probably due to the change in reaction medium when [MeI] is varied from 0.8 to 4 M (corresponding to 5−25% v/v MeI in CH_2Cl_2). In view of this, the value of k_b ((2.4

(20) Chianese, A. R.; Li, X.; Janzen, M. C.; Faller, J. W.; Crabtree, R. H. *Organometallics* **2003**, *22*, 1663.
(21) Adams, H.; Bailey, N. A.; Mann, B. E.; Manuel, C. P. *Inorg. Chim. Acta* **1992**, *198−200*, 111. Gonsalvi, L.; Adams, H.; Sunley, G. J.; Ditzel, E.; Haynes, A. *J. Am. Chem. Soc.* **2002**, *124*, 13597. Søtofte, I.; Hjortkjaer, J. *Acta Chem. Scand.* **1994**, *48*, 872.
(22) Moloy, K. G.; Petersen, J. L. *Organometallics* **1995**, *14*, 2931.
(23) Gonsalvi, L.; Gaunt, J. A.; Adams, H.; Castro, A.; Sunley, G. J.; Haynes, A. *Organometallics* **2003**, *22*, 1047.

Table 1. Rate and Equilibrium Constants for Reaction of MeI with 3a in CH_2Cl_2

T/K	[MeI]/M	$10^4\ k_{obs}/s^{-1}$	K_e/M^{-1}	$10^4 k_f/M^{-1}\ s^{-1}$ [a]	$10^5 k_b/s^{-1}$ [a]	$10^5 k_b/s^{-1}$ [b]
288	1.6	3.94	8.02	2.29	2.85	
293	1.6	5.26	5.00	2.93	5.85	6.61
298	0.8	4.52	4.43	4.41	9.94	
298	1.6	7.31	3.89	3.94	10.1	12.1
298	2.4	9.8	3.79	3.68	9.71	
298	3.2	11.8	3.75	3.41	9.09	
298	4.0	13.8	3.55	3.22	9.09	
303	1.6	9.86	2.74	5.01	18.5	22.6
308						39.3
313						62.5

[a] Calculated from k_{obs} and K_e values using eq 3. [b] Measured directly for reversion of **5a** to **3a**.

$\pm$ 0.2) $\times$ 10^{-4} s^{-1}) obtained from the intercept is not considered very reliable.[24]

The equilibrium constant K_e for eq 1 could also be obtained from the FTIR data using the ratio $\{(A_o - A_e)/A_e[MeI]\}$ where A_o and A_e are the initial and equilibrium absorbances of the 1943 cm^{-1} ν(CO) band of **3a**. Values of K_e obtained in this manner are listed in Table 1. A vant Hoff plot of the variable-temperature data (at [MeI] = 1.6 M) gave thermodynamic parameters $\Delta H = -51 \pm 3$ kJ mol^{-1} and $\Delta S = -159 \pm 12$ J mol^{-1} K^{-1}. Thus the reaction described by eq 1 is exothermic but disfavored entropically, as expected for an addition reaction. K_e tended toward slightly lower values at high [MeI], which can, again, be ascribed to a medium effect.

Since K_e is equal to the ratio k_f/k_b, eq 2 can be modified to give k_f in terms of k_{obs} and K_e (eq 3).

$$k_f = k_{obs}/([MeI] + 1/K_e) \qquad (3)$$

Combination of the measured k_{obs} and K_e data enabled calculation of k_f and k_b, values for which are listed in Table 1. Eyring plots of the k_f data gave activation parameters $\Delta H^{\ddagger} = 36 \pm 1$ kJ mol^{-1} and $\Delta S^{\ddagger} = -189 \pm 3$ J mol^{-1} K^{-1}. Although these parameters are typical for oxidative addition of MeI to Rh(I), proceeding via an S_N2-type mechanism, it should be remembered that k_f represents the *net* rate constant for the forward reaction and may actually contain contributions from both oxidative addition and migratory insertion steps, depending on their relative rates.

The reverse rate constant k_b was also measured *directly* by following the conversion of **5a** back into **3a**. As for the in situ NMR experiment described above, samples containing predominantly (>95%) **5a** were prepared by reaction of **3a** with neat MeI, which was removed in vacuo. The residue was then dissolved in CH_2Cl_2 and the solution monitored by FTIR spectroscopy. Exponential decay of the ν(CO) band of **5a** showed the reverse reaction to be first order in [**5a**] and provided the values of k_b listed in the final column of Table 1. These values are in good agreement with those obtained indirectly from K_e and k_{obs} using eq 3. Activation parameters derived from Eyring plots of the two sets of k_b data are insignificantly different from each other ($\Delta H^{\ddagger} = 87 \pm 3$ kJ mol^{-1} and $\Delta S^{\ddagger} = -30 \pm 10$ J mol^{-1} K^{-1} (indirect method) or $\Delta H^{\ddagger} = 84 \pm 2$ kJ mol^{-1} and $\Delta S^{\ddagger} = -38 \pm 6$ J mol^{-1} K^{-1} (direct method)).

Comparison with Phosphine Analogues. Kinetic studies have been reported for oxidative addition of MeI to a number of Rh(I) Vaska complexes of the type [Rh(CO)$(PR_3)_2$X].[25,26] When PR_3 is a trialkyl phosphine, relatively fast addition of MeI gives isolable Rh(III) methyl complexes [Rh(CO)$(PR_3)_2$MeXI]. For triaryl phosphines, oxidative addition is slower and subsequent migratory CO insertion leads to acetyl complexes, [Rh$(PR_3)_2$(COMe)XI].

Since the donor abilities of NHC ligands and trialkyl phosphines are often compared, it is informative to compare the present results with those reported by Rankin et al. for the reaction of [Rh(CO)$(PEt_3)_2$I] with MeI.[26] The most striking difference between the two systems is in the nature and stability of the products obtained. Addition of MeI to [Rh(CO)$(PEt_3)_2$I] gives a stable octahedral Rh(III) methyl complex, [Rh(CO)$(PEt_3)_2I_2$Me], whereas reaction of **3a** with MeI leads to an equilibrium with the Rh(III) acetyl complex, **5a**. The presumed intermediate methyl complex, **4a**, must only be present at a small concentration to avoid detection by IR spectroscopy.[27]

The rate constant for MeI oxidative addition to [Rh(CO)$(PEt_3)_2$I] reported by Rankin et al. is 1.37×10^{-3} M^{-1} s^{-1} (25 °C, CH_2Cl_2), which is ca. 3.5 times larger than our value of k_f measured under the same conditions for **2b**. Thus, despite the greater electron density on the Rh(I) center of **3a** (ν(CO) 1943 cm^{-1}) compared with [Rh(CO)$(PEt_3)_2$I] (ν(CO) 1961 cm^{-1}), its nucleophilicity toward MeI is lower.

The different reactivity displayed by **3a** and [Rh(CO)$(PEt_3)_2$I] toward MeI can be explained by steric effects exerted by the NHC ligands in **3a**. An X-ray crystal structure of the chloride analogue, **2a** (obtained by Herrmann et al.[17]), is shown in Figure 3. The NHC ligands adopt a conformation with their planes inclined significantly from the metal coordination plane (Cl−Rh−C−N torsion angles ca. 70°). Similar conformations are found in crystal structures of **1a** and **1c**, which display even larger Cl−Rh−C−N torsion angles of ca. 80−85°.[15] It is clear from these structures that the *N*-alkyl substituents of the NHC ligands are placed above and below the Rh coordination plane and cause

(24) A second-order polynomial fit, $k_{obs} = a + b[MeI] + c[MeI]^2$, gave values of $a = (1.4 \pm 0.2) \times 10^{-4}$ s^{-1}; $b = (4.1 \pm 0.2) \times 10^{-4}$ M^{-1} s^{-1}; $c = (-2.5 \pm 0.5) \times 10^{-5}$ M^{-2} s^{-1} ($R = 0.999$).

(25) Franks, S.; Hartley, F. R.; Chipperfield, J. R. *Inorg. Chem.* **1981**, *20*, 3238. Douek, I. C.; Wilkinson, G. *J. Chem. Soc. (A)* **1969**, 2604.

(26) Rankin, J.; Benyei, A. C.; Poole, A. D.; Cole-Hamilton, D. J. *J. Chem. Soc., Dalton Trans.* **1999**, 3771. Rankin, J.; Poole, A. D.; Benyei, A. C.; Cole-Hamilton, D. J. *Chem. Commun.* **1997**, 1835.

(27) A weak IR band at 2073 cm^{-1} observed during the reaction of **3a** with MeI in CH_2Cl_2 may be due to a small concentration of a Rh(III) methyl intermediate. In experiments carried out in acetontrile, a more intense band was observed at similar frequency (2067 cm^{-1}). The large shift in ν(CO) (relative to **3a**, 1943 cm^{-1}) may indicate formation of an ionic intermediate, $[Rh(CO)(L_{Me})_2MeI]^+I^-$, by S_N2 attack of **3a** on MeI. Such a species might be stabilized by a polar coordinating solvent. Further investigation of this behavior is in progress.

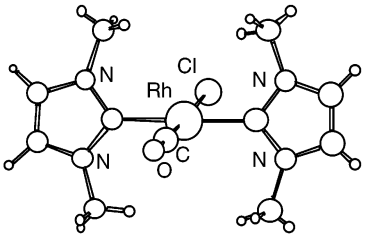

Figure 3. Molecular structure of $[Rh(CO)(L_{Me})_2Cl]$ from X-ray structure reported by Hermann et al.[17]

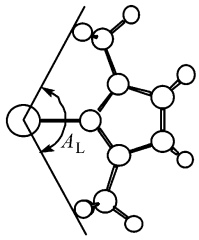

Figure 4. Measurement of the steric parameter A_L, illustrated for the Rh-L_{Me} fragment.

significant steric congestion of the vacant axial coordination sites. Thus, the *N*-methyl groups of **3a** will inhibit nucleophilic attack by the Rh(I) center on MeI, explaining the lower reactivity compared with $[Rh(CO)(PEt_3)_2I]$. This explanation also accounts for the complete lack of reactivity of **3f** with MeI, since steric effects will be even more pronounced on replacing the NHC methyl substituents with mesityls.

As well as moderating the nucleophilicity of **3a**, steric congestion evidently destabilizes the octahedral methyl complex **4a**. This provides a driving force for migratory CO insertion, since a decrease in coordination number from six to five will partially relieve steric congestion around the metal. Despite this, the acetyl product, **5a**, must still be significantly destabilized by steric effects, since reversion to **3a** by elimination of MeI occurs readily under ambient conditions. A recent study in our laboratories of the reactivity of chelate complexes, $[Rh(CO)(\alpha\text{-diimine})I]$, also revealed pronounced steric effects on the kinetics and thermodynamics of MeI oxidative addition and migratory CO insertion.[23] Increased steric bulk (introduced via ortho-substitution of *N*-aryl groups on the diimine ligands) was found to inhibit oxidative addition, but to favor CO insertion. Appropriate choice of ligand enabled isolation and structural characterization of examples of both octahedral methyl and square-pyramidal acetyl complexes.

For phosphine ligands, Tolman's cone angle and electronic parameter (TEP) have found wide utility in the analysis of stereoelectronic effects.[28] The TEP is given by the frequency of the A_1 ν(CO) vibration of $[Ni(CO)_3(L)]$ and has a value of 2061.7 cm^{-1} for PEt_3. The complex $[Ni(CO)_3(L_{Me})]$ is reported to have ν(CO) 2055 cm^{-1}, consistent with stronger electron donation by the NHC ligand.[29] A value of TEP for L_{Me} (2054.4 cm^{-1}) derived recently from quantum chemical calculations[30] matches the experimental value closely. Wilson et al. incorporated these parameters in the QALE method to analyze the rates of MeI oxidative addition to iridium Vaska complexes, $[Ir(CO)(L)_2Cl]$.[31] If it is assumed that the trend for phosphine ligands can be extended to NHC ligands and that ligand electronic effects are similar on Rh(I) and Ir(I), then the difference in TEP between PEt_3 and L_{Me} would predict faster oxidative addition of MeI to **3a** than to $[Rh(CO)(PEt_3)_2I]$ by a factor of ca. 100. Since **3a** actually reacts with MeI ca. 3.5 times *slower* than $[Rh(CO)(PEt_3)_2I]$, it can be estimated that the different steric properties of PEt_3 and L_{Me} result in a lowering of oxidative addition rate by a factor of $>10^2$.

Scheme 3. Reductive Elimination Reactions of Pd(II)-NHC Complexes (R′ = alkyl, acyl)

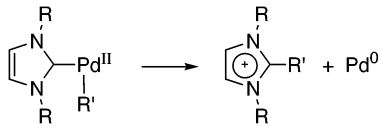

While the Tolman cone angle is not appropriate to describe the steric environment generated by NHC ligands coordinated to a metal, it has been suggested that two steric parameters, A_L and A_H, can be used to represent the "length" and "height" of this type of ligand.[5,7,32] For the ligand conformation adopted in square-planar complexes such as **3a**, the important parameter is A_L, illustrated in Figure 4. From crystallographic data for Rh complexes, we estimate that A_L takes a value of ca. 150° for L_{Me} and ca. 180° for L_{Mes}.[33] Although these values cannot be compared directly with the cone angles of phosphines (e.g., $\theta = 132°$ for PEt_3), they do demonstrate the substantial out-of plane steric bulk for NHC ligands in square-planar complexes.

Reactivity of the Rh−NHC Bonds. It has recently been demonstrated that Pd(II) complexes containing both NHC and alkyl (or acyl) ligands can undergo reductive elimination to generate imidazolium cations (Scheme 3).[10,34] Although the same opportunity arises for the Rh(III) acetyl complex **5a** (and reactive intermediate **4a**), reductive elimination of MeI is preferred in the present system. However, when **3a** was treated with HCl in THF, the formation of additional ν(CO) bands at 2074 and 2001 cm^{-1} indicated partial conversion of **3a** into a monocarbene product $[Rh(CO)_2(L_{Me})X]$ (X = I or Cl). Thus, a Brønsted acid can induce loss of an NHC ligand, presumably by protonation, to give the imidazolium cation (either directly or via an intermediate Rh(III) hydride). Redistribution of CO ligands between Rh centers is also necessary to attain the observed product.

Oxidative addition of H_2 could also be envisaged as a route to reductive elimination of an NHC ligand. However, no reaction was detectable (by in situ high-pressure IR spectroscopy) when a solution of **3a** in CH_2Cl_2 was subjected to 20 atm H_2 at room temperature.

(28) Tolman, C. A. *Chem. Rev.* **1977**, *77*, 313.
(29) Oefele, K.; Herrmann, W. A.; Mihalios, D.; Elison, M.; Herdtweck, E.; Scherer, W.; Mink, J. *J. Organomet. Chem.* **1993**, *459*, 177.
(30) Perrin, L.; Clot, E.; Eisenstein, O.; Loch, J.; Crabtree, R. H. *Inorg. Chem.* **2001**, *40*, 5806.
(31) Wilson, M. R.; Liu, H.; Prock, A.; Giering, W. P. *Organometallics* **1993**, *12*, 2044.
(32) Jafarpour, L.; Nolan, S. P. *J. Organomet. Chem.* **2001**, *617−618*, 17.
(33) The method used here for estimating A_L differs from that in refs 5, 7, and 32, where hydrogen atoms on the *N*-alkyl substituents were not considered. Our values of A_L for L_{Me} and L_{Mes} take into account the hydrogen van der Waals radius, as in cone angle calculations for phosphines.
(34) McGuinness, D. S.; Cavell, K. J. *Organometallics* **2000**, *19*, 4918.

This behavior resembles the low reactivity toward H_2 of $[Rh(CO)(PR_3)_2X]$ complexes.[35]

Catalytic Carbonylation Tests. Since oxidative addition of MeI to Rh(I) is a key reaction in the catalytic cycle for the carbonylation of methanol, we tested the catalytic properties of **3a**. Experiments were conducted using a high-pressure infrared cell to monitor the reaction in situ. A solution of **3a** (12 mM) in chlorobenzene containing 10% methanol and 2% MeI (v/v) was heated to 120 °C under 10 atm CO. Under these conditions the IR spectrum initially displayed absorptions at 2073 and 1999 cm^{-1}, consistent with the dicarbonyl complex $[Rh(CO)_2(L_{Me})I]$ (also observed as an intermediate during the synthesis of **3a**, and on reaction of **3a** with HCl, vide supra). These bands then decayed (over 1−2 h) to be replaced by absorptions at 2058 and 1989 cm^{-1}, which correspond to $[Rh(CO)_2I_2]^-$, the conventional "Monsanto catalyst". Thus, the NHC ligands are lost from the Rh center sequentially under the applied conditions (which are much milder than those used for commercial methanol carbonylation). Catalytic activity was monitored by following the growth of a band at 1746 cm^{-1} due to methyl acetate, resulting from esterification of acetic acid in the presence of excess methanol. Initially (when the main Rh species was $[Rh(CO)_2(L_{Me})I]$), the formation of methyl acetate was very sluggish, indicating that that the mono-NHC complex is not particularly active. However, on loss of the second L_{Me} ligand and conversion to $[Rh(CO)_2I_2]^-$, the catalytic rate increased and reached a peak (76 mmol dm^{-3} h^{-1}) similar to that measured (89 mmol dm^{-3} h^{-1}) in a control reaction using $Bu_4N[Rh(CO)_2I_2]$ as the catalyst. Thus we found no evidence that coordination of L_{Me} ligands enhances carbonylation activity. We have not examined the mechanism by which the L_{Me} ligands dissociate from the Rh center, but protonation, methylation, and acetylation at C-2 of the heterocycle to give imidazolium cations are all possibilities.

Structural Characterization of a Bis(carbene) Rh(III) Acetate Complex. On prolonged standing, solutions remaining from kinetic studies of the reaction of **3a** with MeI in CH_2Cl_2 were found to yield dark crystals, one of which was selected for an X-ray diffraction study. The resulting structure, shown in Figure 5, reveals a Rh(III) complex of formula $[Rh(L_{Me})_2I_2(OAc)]$ (**6a**). The iodide ligands are mutually trans (I−Rh−I angle 172°), whereas the L_{Me} ligands are mutually cis (C−Rh−C angle 94°). The two remaining sites in the pseudo-octahedral coordination sphere are occupied by a chelating bidentate acetate ligand. The complex has C_2 symmetry with the Rh atom and C−C bond of the acetate ligand lying on the rotation axis. The two L_{Me} ligands take up a conformation such that the steric interaction between their N-Me groups (and with the iodide ligands) is minimized. Although **6a** is the first structure of this type containing monodentate NHC ligands, a number of analogous Rh(III) and Ir(III) complexes containing cis-chelating bidentate NHC ligands have been reported recently.[36] The geometrical features of **6a** closely resemble the chelate analogues, the most notable difference being a slightly wider C−Rh−C bond angle for **6a**. It is of interest that the NHC ligands in **6a** are cis, despite the absence of a chelate bridge, which suggests an inherent preference for this geometry.

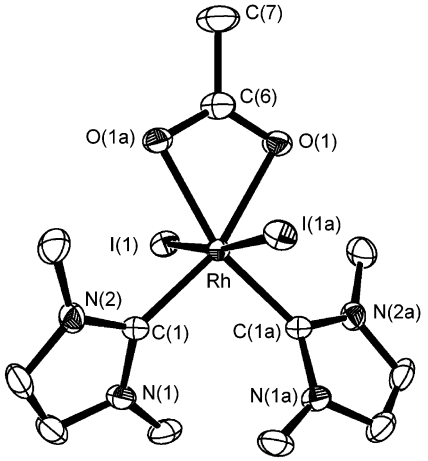

Figure 5. ORTEP plot for **6a**. Thermal ellipsoids are shown at the 50% probability level. Hydrogen atoms are omitted for clarity. Selected bond lengths (Å): Rh−C 1.997(4), Rh−I 2.6753(4), Rh−O 2.173(3), O−C(6) 1.258(4), C(6)−C(7) 1.508(9), C(1)−N(1) 1.372(5), C(1)−N(2) 1.360(5). Angles (deg): I(1)−Rh−I(1a) 172.42(2), C(1)−Rh−C(1a) 94.3(2), C(1)−Rh−I(1) 87.02(12), C(1)−Rh−I(1a) 98.16(12), O(1)−Rh−O(1a) 60.20(16), I(1)−Rh−O(1) 88.85(9), I(1)−Rh−O(1a) 84.60(9), C(1)−Rh−O(1) 162.85(15), C(1)−Rh−O(1a) 102.81(15), N(1)−C(1)−N(2) 104.4(4), Rh−C(1)−N(1) 132.0(3), Rh−C(1)−N(2) 123.4(3).

Scheme 4. Proposed Mechanism for Formation of 6a

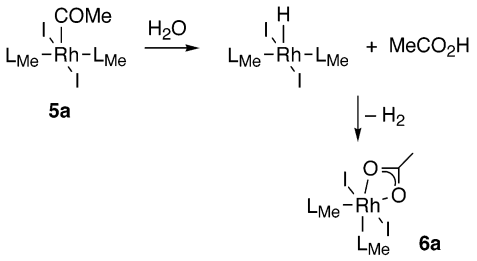

The acetate ligand in **6a** most likely derives from the acetyl ligand in **5a**. A slow reaction of **5a** with adventitious water could lead to **6a** by the reaction sequence shown in Scheme 4. Hydrolysis of the Rh−COMe bond would lead to a Rh(III) hydride and acetic acid (a reaction that occurs in a related phosphine system[22]). Elimination of H_2 (by protonation of the hydride) and coordination of acetate would give the observed product.[37]

Conclusions

Despite the high electron density bestowed upon the Rh center of **3a** by the pair of NHC ligands, its nucleophilicity toward MeI is significantly diminished by the steric bulk of the ligand *N*-methyl substituents.

(35) Morran, P. D.; Duckett, S. B.; Howe, P. R.; McGrady, J. E.; Colebrooke, S. A.; Eisenberg, R.; Partridge, M. G.; Lohman, J. A. B. *J. Chem. Soc., Dalton Trans.* **1999**, 3949.

(36) Albrecht, M.; Miecznikowski, J. R.; Samuel, A.; Faller, J. W.; Crabtree, R. H. *Organometallics* **2002**, *21*, 3596. Albrecht, M.; Crabtree, R. H.; Mata, J.; Peris, E. *Chem. Commun.* **2002**, 32. Poyatos, M.; Sanaú, M.; Peris, E. *Inorg. Chem.* **2003**, *42*, 2572.

(37) Syntheses reported for the analogous chelate complexes $[M(bis\text{-}NHC)I_2(OAc)]$ involve reaction of $[M(cod)Cl]_2$ with NaOAc and KI and therefore require oxidation of the metal center from M(I) to M(III). This oxidation may also involve evolution of H_2 (ref 36).

The octahedral product of MeI addition is also destabilized by steric effects, such that both reductive elimination of MeI and migratory CO insertion to give the acetyl **5a** are facile. Both kinetic and thermodynamic parameters have been measured for the reaction **3a** + MeI = **5a**. Our results allow a direct comparison of the influence of phosphine and NHC ligands on two important classes of organometallic reaction. It is clear that the steric constraints created by the *N*-alkyl substituents of NHC ligands can have a dramatic influence on reactivity and can be large enough to reverse the trend in reactivity predicted on the basis of ligand electronic properties. Although NHC ligands are often suggested to mimic the properties of trialkylphosphines, these results emphasize that the influence of their high donor strength can be significantly moderated by steric effects.

Experimental Section

Materials. All solvents used for synthesis or kinetic experiments were distilled and degassed prior to use following literature procedures.[38] Synthetic procedures were carried out utilizing standard Schlenk techniques. Nitrogen and carbon monoxide were dried through a short (20 × 3 cm diameter) column of molecular sieves (4 Å) which was regularly regenerated. Carbon monoxide was also passed through a short column of activated charcoal to remove any iron pentacarbonyl impurity.[39] The Rh precursor $[Rh(CO)_2Cl]_2$[40] and 1,3-dimethylimidazolium iodide[41] were synthesized according to literature procedures. Methyl iodide (Aldrich) was distilled over calcium hydride and stored in foil-wrapped Schlenk tubes under nitrogen and over mercury to prevent formation of I_2. *N*-Methylimidazole, NaOAc, Cs_2CO_3, CsI, (Aldrich), 1,3-dimesitylimidazolium chloride, $[Rh(CO)_2(acac)]$ (Strem), and $RhCl_3 \cdot xH_2O$ (PMO) were used as supplied.

Instrumentation. Ambient-pressure FTIR spectra (2 cm^{-1} resolution) were measured using a Mattson Genesis Series spectrometer, controlled by WINFIRST software running on a Viglen 486 PC. In situ high-pressure FTIR spectra were measured using a SpectraTech cylindrical internal reflectance (CIR) cell and a Perkin-Elmer 1710 spectrometer fitted with an MCT detector. ^1H NMR spectra were obtained using a Bruker AC250 spectrometer fitted with a Bruker B-ACS60 automatic sample changer operating in pulse Fourier transform mode, using the solvent as reference. Elemental analyses were performed using a Perkin-Elmer 2400 elemental analyzer.

Synthesis of Rh(I) Complexes. (a) $[Rh(CO)_2(OAc)]_2$.[42] Pentane (50 cm^3), presaturated with CO, was added to a mixture of $[Rh(CO)_2Cl]_2$ (0.521 g, 1.34 mmol) and NaOAc (0.809 g, 9.86 mmol) under a CO atmosphere at room temperature. The mixture was stirred for 18 h and then filtered to remove sodium salts. The solvent was removed in vacuo, and the solid residue purified by vacuum sublimation to give a red-green dichroic crystalline solid; yield 0.447 g (77%). IR (CH_2Cl_2 ν(CO)/cm^{-1}): 2073, 2022.

(b) $[Rh(CO)(L_{Me})_2I]$, 3a. $[Rh(CO)_2(OAc)]_2$ (0.200 g, 0.46 mmol), 1,3-dimethylimidazolium iodide (0.41 g, 1.83 mmol), and Cs_2CO_3 (0.537 g, 1.65 mmol) were placed in a 100 cm^3 Schlenk flask under N_2. THF (80 cm^3) was added, and the mixture was stirred overnight at 50 °C. A color change from brown to yellow was observed. Insoluble byproducts were removed by filtration through a short silica column. The solvent was removed in vacuo and the product purified by recrystallization from a minimum amount of THF and addition of excess pentane. The yellow solid was then dried in vacuo overnight; yield 0.189 g (46%). An alternative method using $[Rh(acac)(CO)_2]$ as the source of rhodium and the same reaction conditions and workup afforded the same product in similar yield. Anal. Calcd for $C_{11}H_{16}IN_4ORh$: C, 29.4; H, 3.6; N, 12.5. Found: C, 29.6; H, 3.6; N, 12.2. IR (CH_2Cl_2; ν(CO)/cm^{-1}): 1943. ^1H NMR (CD_2Cl_2; δ): 3.95 (s, 12H, N*Me*), 6.96 (s, 4H, NC*HCH*N).

(c) $[Rh(CO)(L_{Mes})_2I]$, 3f. The preparation was carried out on a small scale for spectroscopic characterization of **3f**. $[Rh(CO)_2(OAc)]_2$ (10.4 mg, 23.9 μmol), 1,3-dimesitylimidazolium chloride (31.3 mg, 91.8 μmol), Cs_2CO_3 (0.1 g 0.30 mmol), and CsI (0.6 g, 2.3 mmol) were placed in a 50 cm^3 Schlenk flask under N_2. THF (10 cm^3) was added, and the mixture was stirred overnight at 50 °C. After filtration through a short silica column, the solvent was removed in vacuo. IR (CH_2Cl_2; ν(CO)/cm^{-1}): 1937. ^1H NMR (CD_2Cl_2; δ): 1.76, 2.05 (each s, 12H, mesityl 2,6-CH_3), 2.44 (s, 12H, mesityl 4-CH_3), 6.87 (s, 4H NC*HCH*N), 6.89 (br, 8H mesityl 3,5-*H*).

X-ray Structure Determination. Data for complex **6a** were collected on a Bruker Smart CCD area detector with Oxford Cryosystems low-temperature system using Mo Kα radiation ($\bar{\lambda}$ = 0.71073 Å). The structure was solved by Patterson synthesis and refined by full matrix least-squares methods on F^2. Hydrogen atoms were placed geometrically and refined using a riding model (including torsional freedom for methyl groups). Complex scattering factors were taken from the SHELXTL program package[43] as implemented on the Viglen Pentium computer. Crystallographic data are summarized in Table 2, and full listings of data are given in the Supporting Information.

Table 2. Summary of Crystallographic Data for Complex 6a

formula	$C_{12}H_{19}I_2N_4O_2Rh$
fw	608.02
cryst syst	monoclinic
space group	*C*2/*c*
color	black
a (Å)	9.0651(10)
b (Å)	13.5202(14)
c (Å)	14.6174(16)
α (deg)	90
β (deg)	105.184(2)
γ (deg)	90
temp (K)	150(2)
Z	4
final *R* indices [$I > 2\sigma(I)$]	R1 = 0.0393; wR_2 = 0.1047
R indices (all data)	R1 = 0.0424; wR_2 = 0.1073
GOF	1.078

Kinetic Experiments. For the oxidative addition reaction, **3a** + MeI → **5a**, the required amount of freshly distilled methyl iodide was placed in a 5 cm^3 graduated flask, which was then made up to the mark with the solvent of choice (usually CH_2Cl_2). A portion of this solution was used to record a background spectrum. Another portion (typically 500 μL) was added to the solid complex **3a** (typically 5−8 μmol) in a sample vial to give a reaction solution containing 10−15 mM [Rh]. A portion of the reaction solution was quickly transferred to the IR cell, and the kinetic experiment was started. Pseudo-first-order conditions were employed, with at least a 50-fold excess of MeI, relative to the metal complex. The IR cell (0.5 mm path length, CaF_2 windows) was maintained at constant temperature throughout the kinetic run by a thermostated jacket. Spectra were scanned in the metal carbonyl ν(CO) region (2200−1600 cm^{-1}) and saved at regular time intervals under computer

(38) Perrin, D. D.; Armerego, W. L. F.; Perrin, D. R. *Purification of Laboratory Chemicals*, 3rd ed.; Pergamon Press: Oxford, 1988.
(39) Haynes, A.; Ellis, P. R.; Byers, P. K.; Maitlis, P. M. *Chem. Br.* **1992**, *28*, 517.
(40) McCleverty, J.; Wilkinson, G. *Inorg. Synth.* **1966**, *8*, 214.
(41) Herrmann, W. A.; Köcher, C.; Goossen, L. J.; Artus, G. R. J. *Chem. Eur. J.* **1996**, *2*, 1627.
(42) Lawson, D. N.; Wilkinson, G. *J. Chem. Soc.* **1965**, 1900.
(43) Sheldrick, G. M. *SHELXTL, An integrated system for solving and refining crystal structures from diffraction data*, revision 5.1; Bruker AXS Ltd.: Madison, WI.

control. After the kinetic run, absorbance versus time data for the appropriate ν(CO) frequencies were extracted and analyzed off-line using Kaleidagraph curve-fitting software. The decay of the band of **3a** was well fitted by an exponential curve with correlation coefficient ≥ 0.999, to give a pseudo-first-order rate constant. Each kinetic run was repeated at least twice to check reproducibility, the k_{obs} values given being averaged values with component measurements deviating from each other by $\leq 5\%$.

For the reverse reaction, a sample of **5a** was prepared initially by dissolving complex **3a** (10−20 mg) in neat MeI and stirring the solution under N_2 for 1.5 h. The MeI was then removed in vacuo to give **5a** as a dark red solid. IR (ν(CO)/cm^{-1}): 1697. ^{1}H NMR (CD_2Cl_2; δ): 7.03, 6.97 (each d, 2H, NC*H*C*H*N) 3.93, 3.73 (each s, 6H, N*Me*), 3.17 (s, 3H, CO*Me*). Solutions of **5a** in CH_2Cl_2 were monitored by IR spectroscopy as described above to determine the kinetics for the reaction **5a** → **3a** + MeI. The same reaction was also monitored in CD_2Cl_2 by ^{1}H NMR spectroscopy

Acknowledgment. This work was supported by BP Chemicals Ltd (studentship to J.A.G.), EPSRC, and the University of Sheffield.

Supporting Information Available: Crystallographic data (PDF and CIF). This material is available free of charge via the Internet at http://pubs.acs.org.

OM034022G